

## The latest status of LHC and the EWSB physics

S. Asai

*Physics Department, University of Tokyo, Hongo Bunkyo-ku Tokyo 133-033 Japan,  
Shoji.Asai@cern.ch*

The latest status of LHC and the performances of ATLAS and CMS detectors are summarized in the first part. Physics potential to solve the origin of the ElectroWeak Symmetry Breaking is summarized in the 2nd part, focusing especially on two major scenarios, (1) the light Higgs boson plus SUSY and (2) the Strong Coupling Gauge Theory. Both ATLAS and CMS detectors have the excellent potential to discover them, and we can perform crucial test on the ElectroWeak Symmetry Breaking.

*Keywords:* LHC, Higgs, SUSY, Technicolor

### 1. Introduction

The most urgent and important topics of the particle physics is to understand the electroweak symmetry breaking and the origin of "Mass". These are the main purpose of the Large Hadron Collider (LHC). The LHC accelerator is composed with 1232 units of the 8.4 T superconducting dipole magnet (length is 14.2 m each) and 392 units of the quadruple magnet. They have already be arranged in the 26.6 km circumference tunnel. Protons will be accelerated upto 7 TeV and collide each other, Thus the center-of-mass energy( $\sqrt{s}$ ) of  $pp$ -system is 14 TeV. The first physics collisions have been observed in 2009 with the lower  $\sqrt{s}$ 's of 900 GeV and 2.36 TeV. The design luminosity is  $10^{34}cm^{-2}s^{-1}$ , which corresponds to  $100\text{ fb}^{-1}$  per year, will be achieved at 2015.

The production cross-sections are expected to be large at LHC for the various high  $p_T$  and high mass elementary processes as listed in Table 1, since gluon inside partons can contribute remarkably. Furthermore, because the LHC provides the high luminosity of  $10\text{--}100\text{ fb}^{-1}$  per year, large numbers of the interesting events will be observed. LHC has an excellent potential to produce high mass particles, for example, the top quark, the Higgs boson, SUSY particles.

### 2. Status and Future plan of LHC

#### 2.1. Incident on 19th September 2008

The LHC has started on 10th September 2008. Protons were injected with the energy of 450GeV and were RF-captured successfully to store in the LHC ring. But there were the bad connections of the splicing in the copper bar between magnet

	$\sigma$ (pb at 14TeV)	Event number (L=10 fb <sup>-1</sup> )
$W^\pm \rightarrow \ell^\pm \nu$	$1.7 \times 10^5$	$\sim 10^9$
$Z^0 \rightarrow \ell^+ \ell^-$	$2.5 \times 10^4$	$\sim 10^8$
$t\bar{t}$	830	$\sim 10^7$
$jj$ $p_T > 200\text{GeV}$	$10^5$	$\sim 10^9$
SM Higgs (M=115GeV)	35	$\sim 10^5$
$\tilde{g}\tilde{g}$ (M=500GeV)	$\sim 100$	$\sim 10^6$
(M=1TeV)	$\sim 1$	$\sim 10^4$

units. The copper bar becomes the path of intense current ( $\sim 10000$  A), when the superconducting in the magnet is quenched. Since the bad connections have the resistance of  $\sim 50\mu\Omega$ , the temperature goes up quickly and the liquid He boils up. Total 6 ton of the liquid He leaks from the pipe and 53 units of the magnets have been destroyed.

To repair these magnets and to add the various safety systems for the quench (improving the quench detectors, increasing the safety valves, and making the magnet support stronger) it has taken more than one year.

## 2.2. Restart at November 2009

On 20th November 2009, the proton beam makes a turn successfully in the LHC rings and are stored in the beam pipe with the RF power. This test have been performed for both proton beams separately, and the LHC is back to the status before the incident.

On 23rd November, the first collision at  $\sqrt{s}=900$  GeV has been observed in the all detectors and the events observed at the ATLAS and CMS detectors are shown in Fig.1. These events are the soft proton-proton collision, called as "minimum bias". Since the cross-section of minimum bias at 900 GeV is very huge,  $\sigma \sim 58$  mb, large number of the events were observed even with the lower luminosity of  $10^{24}\text{cm}^2\text{s}^{-1}$ . Many soft  $\pi$ 's whose  $p_T$  less than 2 GeV are emitted in the Minimum bias events, and these are useful to check the performance of the detectors as mentioned in Sec.3.

## 2.3. Acceleration and collision at $\sqrt{s}=2.36\text{TeV}$

On 30th November, both beams are accelerated upto 1.18 TeV. Since the beam just after injected has large emittance, the first step of the acceleration is important to control beam. The beam emittance decrease after acceleration, so this success shows that LHC clears the first critical point.

On 8th December, we have the first collision at  $\sqrt{s}=2.36\text{TeV}$ , which is the highest collision energy in the world. The events observed at the ATLAS and CMS detectors

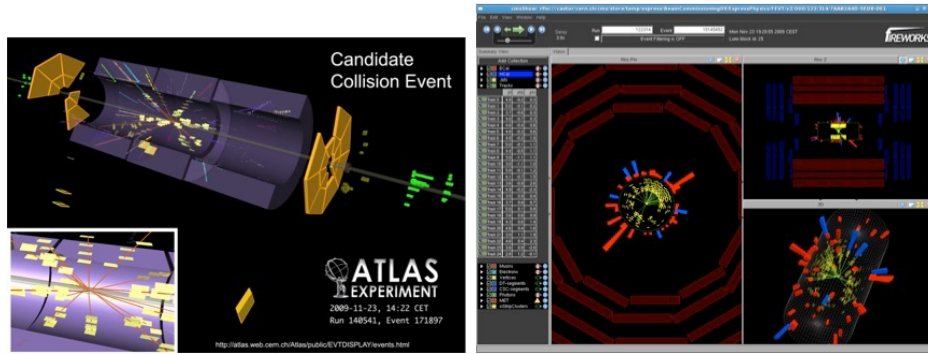


Fig. 1. The collision events at  $\sqrt{s}=900$  GeV observed at ATLAS and CMS

are shown in Fig.2, and these events are multi-jet QCD. The production cross-section and jet-properties measured at both 900 GeV and 2.36 TeV are consistent with the Monte-Carlo predictions, still preliminary.

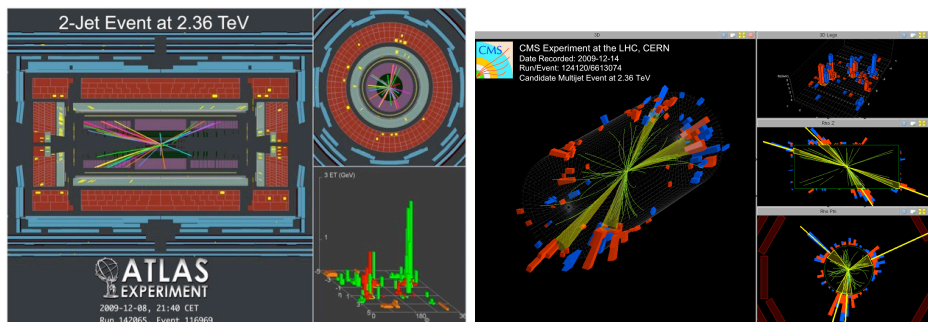


Fig. 2. The collision events at  $\sqrt{s}=2.36$  TeV observed at ATLAS and CMS

#### 2.4. Future plan

The plan of LHC after 2010 is summarized here. There is the high risk when the LHC is operated at  $\sqrt{s}=10$  TeV without the repair of the bad connection of the splicing mentioned in Sec.2.1. Magnet units should be warm in order to repair the connections, and it takes much time more of one year. Thus the LHC schedule is determined as listed in Table 2. LHC will be operated at  $\sqrt{s}=7$  TeV at both 2010 and 2011, and the expected integrated luminosity ( $L$ ) is about  $1 fb^{-1}$  in the forthcoming two years. Physics potentials with these  $\sqrt{s}$  and  $L$  are summarized in Sec.4.

Year	ECM	expected Luminosity
2010	7 TeV	200 $pb^{-1}$
2011	7 TeV	$\sim 1fb^{-1}$
2012	Long shut down	
2013	13-14 TeV	$\sim a few fb^{-1}$
2014	14 TeV	$\sim 10fb^{-1}$

### 3. Status and performance of ATLAS/CMS detector

Two general-purpose experiments exist, ATLAS and CMS, at LHC. The ATLAS (A Toroidal LHC Apparatus) detector measures 22 m high, 44 m long, and weight 7,000 tons. The characteristics of the ATLAS detector are summarized as follows

- Precision inner tracking system is constituted with pixel, strip of silicon and TRT with 2 T solenoidal magnet. Good performance is expected on the  $B$ -tagging and the  $\gamma$ -conversion tagging.
- Liquid Argon electromagnetic calorimeter has fine granularity for space resolution and longitudinal segmentation for fine angular resolution and particle identifications. It has also good energy resolution of about 1.5% for  $e/\gamma$  with energy of 100 GeV.
- Large muon spectrometer with air core toroidal magnet will provide a precise measurement on muon momenta (about 2% for 100 GeV- $\mu$ ) even in the forward region.

The CMS (Compact Muon Solenoid) detector measures 15 m high, 21 m long, and weight 12,500 tons, with the following features

- Precise measurement on high  $p_T$  track is performed with the strong 4 T solenoidal magnet.
- $PbWO_4$  crystal electromagnetic calorimeter is dedicated for  $H_{SM}^0 \rightarrow \gamma\gamma$ .
- High purity identification and precise measurement are expected on  $\mu$  tracks using the compact muon system.

Both detectors are ready to observe the collision events well and the various performance (for example, tracking efficiency, resolution of  $p_T$ , resolution of the energy deposited on the calorimeters) are checked with the collision data at 900 GeV. Some performance plots are shown in Fig.3; Fig.3(a) shows the reconstructed pair of tracks with the displaced vertex for  $K_S \rightarrow \pi^+\pi^-$ , and the distribution of the invariant mass of the reconstructed tracks are shown in Fig.3(b). The clear peak is observed at  $K_s$  mass. These are obtained at the ATLAS detector.  $\pi^0 \rightarrow \gamma\gamma$  is good process to check the EM calorimeters, and the invariant mass distribution of two  $\gamma$ 's is shown in Fig.3(c). Clear peak is observed at  $\pi^0$  mass and the good resolution of  $\sigma=10$  MeV is obtained at the CMS detector, since the  $PbWO_4$  crystal scintillators are used in CMS detector. The  $\cancel{E}_T$  is the vector opposite to the sum of the all

energy deposited on the calorimeters and muon tracks, and is crucial variable to detect neutrino or to discovery SUSY. The  $\cancel{E}_T$  resolution is related to the energy sum deposited on the calorimeters, and it is also checked as shown in Fig.3(d). The resolution is proportional to  $0.5 \times \sqrt{\Sigma E_T}$  and the data is consistent with the MC simulation.

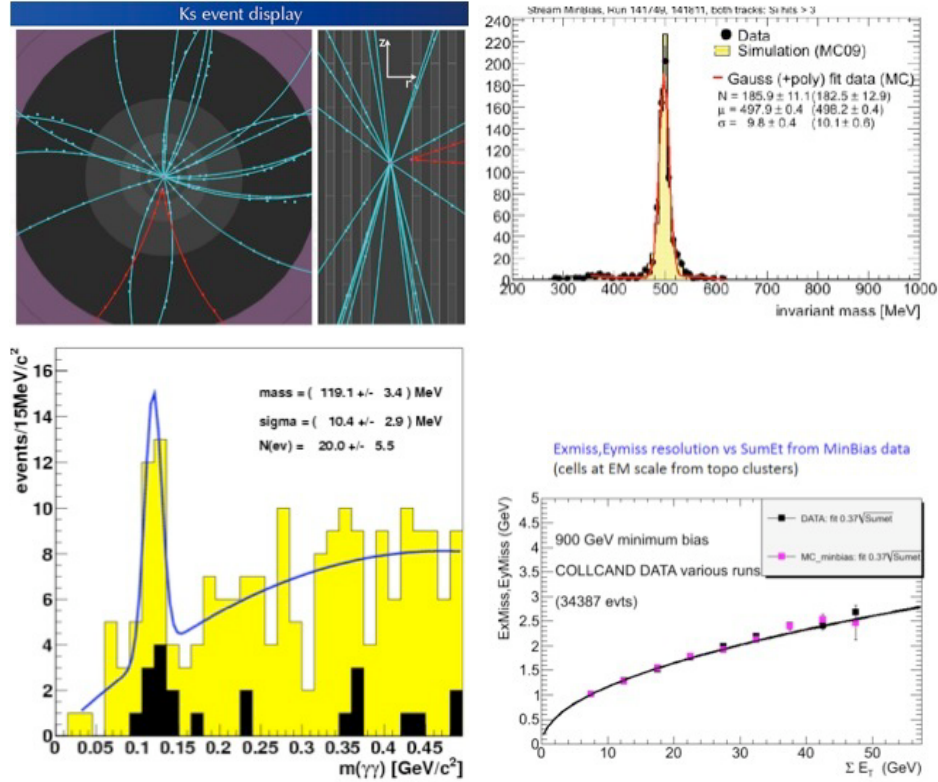


Fig. 3. (a) Event display observed at ATLAS with  $\sqrt{s}=900\text{GeV}$ . The displaced vertex has clearly been reconstructed for  $K_S \rightarrow \pi^+\pi^-$ . (b) The invariant mass distribution of  $\pi^+\pi^-$  pair (ATLAS) (C) The invariant mass distribution of two photons  $\pi^0 \rightarrow \gamma\gamma$  (CMS) (d) The resolution of  $\cancel{E}_T$  as a function of  $\Sigma E_T$

## 4. EWSB scenario 1: Light Higgs and SUSY

### 4.1. $\sqrt{s}$ dependence of the production cross-section $\sigma$

The studies shown in this note are based on  $\sqrt{s}=10$  or 14 TeV. In order to extrapolate these results into  $\sqrt{s}=7$  TeV,  $\sqrt{s}$ -dependences of the production cross-section  $\sigma$  are shown in Figs.4 (a) Higgs (b) SUSY. The production cross-sections at 7 TeV is smaller by factor 3 than  $\sigma$  at 10 TeV, and by factor 5–8 than  $\sigma$  at 14 TeV. The difference becomes larger for the heavier particles.

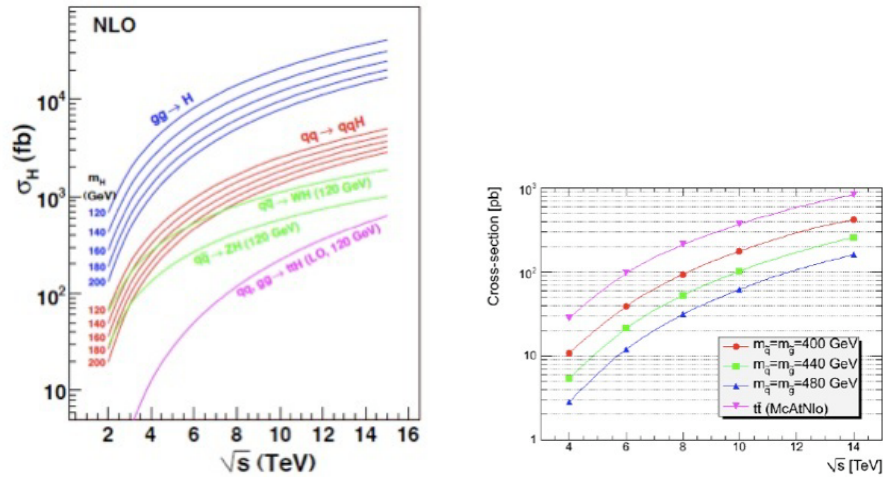


Fig. 4. The production cross-section as a function  $\sqrt{s}$ : (a) The light SM Higgs whose mass 120 to 200 GeV (b) The SUSY particles (gluino, squark masses 400-480 GeV)

#### 4.2. The Light SM Higgs boson

A discovery of one or several Higgs bosons will give a definite experimental proof of the breaking mechanism of the Electroweak gauge symmetry, and detail studies of the Yukawa couplings between the Higgs boson and various fermions will give insights on the origin of lepton and quark masses. The mass of the SM Higgs boson itself is not theoretically predicted, but its upper limit is considered to be about 160 GeV(95%C.L.) from the Electroweak precision measurements and the direct search at the Tevatron. The lower limit of the Higgs boson mass is set at 114 GeV(95%C.L.) by direct searches at LEP. The Higgs boson should exist in the narrow mass range of 114–160 GeV, and lighter than 130 GeV if the Supersymmetry exists.

The SM Higgs boson,  $H_{SM}^0$ , is produced at the LHC predominantly via gluon-gluon fusion(GF) and the second dominant process is vector boson fusion(VBF)  $H_{SM}^0$  decays mainly into  $b\bar{b}$  and  $\tau^+\tau^-$  for the lighter case ( $\gtrsim 130$  GeV). Although its decay into  $\gamma\gamma$ , via the one-loop process including top quark or W boson, is suppressed ( $\sim 2 \times 10^{-3}$ ), this decay mode is very important at the LHC for this light case. On the other hand, it decays into  $W^+W^-$  and  $ZZ$  with a large branching fraction for the heavier case ( $\gtrsim 140$  GeV).

##### 4.2.1. $H_{SM}^0 \rightarrow \gamma\gamma$ in the GF and VBF

This channel is promising for the light Higgs boson, whose mass is lighter than 140 GeV, and this mode indicates the spin of the Higgs boson candidate. Although the branching fraction of this decay mode is small and there is a large background

processes via  $q\bar{q} \rightarrow \gamma\gamma$ , the distinctive features of the signal, high  $p_T$  isolated two photons with a mass peak, allows us to separate the signal from the large irreducible background. The mass resolution of the  $H_{SM}^0 \rightarrow \gamma\gamma$  process is expected to be 1.3 GeV(ATLAS) and 0.9GeV(CMS). Sharp peak appears at Higgs boson mass over the smooth distribution of background events as shown in Fig.5.

VBF provides additional signatures in which two high  $p_T$  jets are observed in the forward regions, and the only two photons from the decay of  $H_{SM}^0$  will be observed in the wide rapidity gap between these jets. The rapidity gap (no jet activity in the central region) is expected because there is no color-connection between two outgoing quarks. These signatures suppress the background contributions significantly as shown in Fig.5(b).

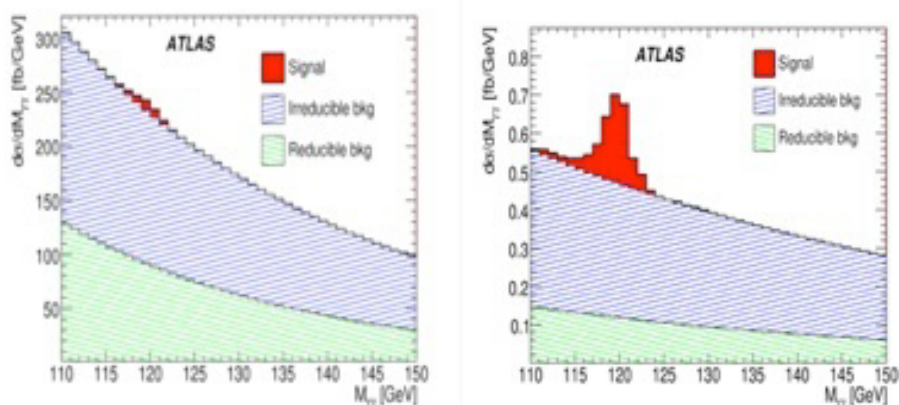


Fig. 5. The invariant mass distribution of  $\gamma\gamma$  (ATLAS).  $H_{SM}^0$  mass is assumed to be 120 GeV. (a) No jet (mainly for GF process) (b) plus 2 jets (for VBF process) In both figures, red histogram shows the signal. Blue and green show the background contributions for real photo and for fake photon, respectively.

#### 4.2.2. $H_{SM}^0 (\rightarrow W^+W^- \rightarrow \ell^\pm\nu\ell^\pm\nu)$ in GF and VBF

The mass range of 130-200 GeV is well covered by the analysis of  $H_{SM}^0 \rightarrow WW \rightarrow \ell\nu\ell\nu$ , both in GF and VBF process. The transverse mass,  $M_T$ , is defined as  $\sqrt{2E_T P_T(\ell\ell)(1 - \cos\phi)}$ , in which  $\phi$  is the azimuthal angle between  $\vec{E}_T$  and  $P_T(\ell\ell)$ . Figure 6 shows the  $M_T$  distribution and a clear Jacobian peak is observed above smooth background distributions. The main background process is  $W^+W^-$  for the topology without-jet (GF)  $t\bar{t}$  for that with two forward jets (VBF). These can be suppressed by using the azimuthal angle correlation between the dileptons because of the following reason. Since the Higgs boson is a spin zero particle, the helicities of the emitted W bosons are opposite. The leptons are then emitted preferably in the same direction due to the 100% parity violation in W decays.

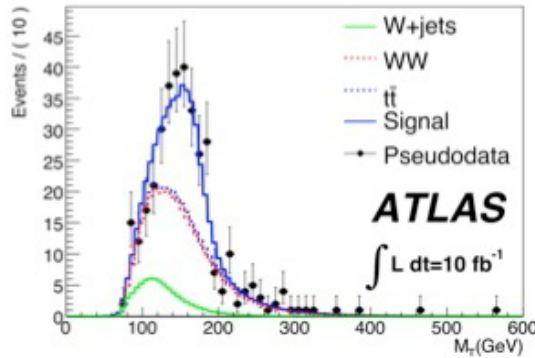


Fig. 6. The transverse mass distribution of  $H_T$  and  $\ell\bar{\ell}$ , in which  $M(H_{SM}^0)=170$  GeV is assumed. Open blue histogram shows the Higgs signal and the red( $W^+W^-$ ) and green( $t\bar{t}$ ) histogram show the background contribution.

#### 4.2.3. $H_{SM}^0 \rightarrow \tau^+\tau^-$ in VBF

$H_{SM}^0 \rightarrow \tau^+\tau^-$  provides high  $p_T$   $\ell^\pm$ , when  $\tau$  decays leptonically, and it can make a clear trigger. Momenta carried by  $\nu$ 's emitted from  $\tau$  decays can be solved approximately by using the  $\cancel{E}_T$  information, and the Higgs mass can be reconstructed (collinear approximation). Figures 7 show the mass distributions of the reconstructed tau-pair for leptonic plus hadronic decays and both leptonic decays. The mass resolutions of about 10 GeV can be obtained, and the signal can be separated from the Z-boson production background. The performance of the  $\cancel{E}_T$  is crucial in this analysis as shown in Fig.3(d). This process provides a direct information on the coupling between the Higgs boson and a fermion, the tau lepton.

#### 4.2.4. $H_{SM}^0 (\rightarrow ZZ \rightarrow \ell^+\ell^-\ell^+\ell^-)$ in GF

The four-lepton channel ( $H_{SM}^0 \rightarrow ZZ \rightarrow \ell^+\ell^-\ell^+\ell^-$ ) is very clean and a sharp mass peak is expected as shown in Figs. 8. Mass resolution of the four lepton system is typically 1%. As shown in Figures, the main background process is ZZ production which gives continuous distribution above 200 GeV. This channel is important for  $H_{SM}^0$  whose mass is heavier than 130 GeV.

#### 4.2.5. Discovery potential $H_{SM}^0$

$5\sigma$ -discovery potential and 98% C.L. exclusion of  $H_{SM}^0$  are summarized in Fig.9 as a function of the Higgs mass. Vertical axis shows the integrated luminosity for discovery and exclusion. The results at ATLAS and CMS are combined. Higgs whose mass is lighter than 130 GeV can be discovered or excluded in 2013 or 2011, respectively. Higgs, heavier 130 GeV, becomes more easy. The Crucial test for light Higgs boson scenario can be performed around 2011-2013.

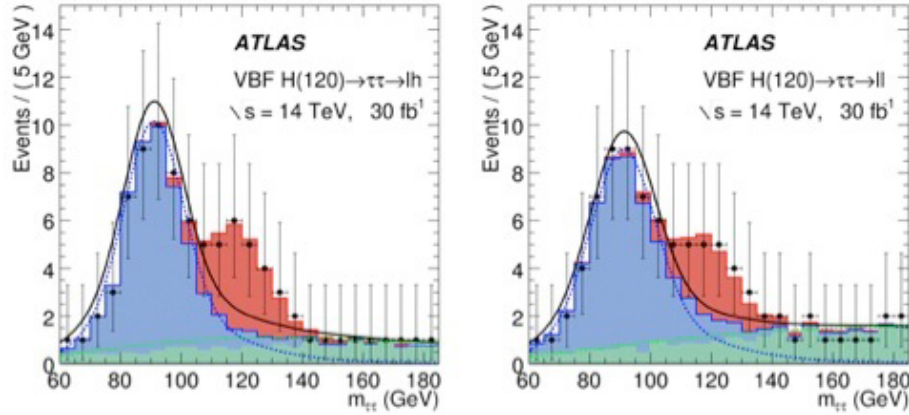


Fig. 7. The invariant mass distributions of  $\tau^+\tau^-$  ( $L=30\text{ fb}^{-1}$  at ATLAS). (a) One tau decays leptonically and another decays hadronically. (b) both tau decays leptonically. In both figures, the red histogram shows the signal with  $M(H_{SM}^0)=120\text{ GeV}$ , and blue( $Z^0 \rightarrow \tau^+\tau^-$ ) and green( $t\bar{t}$ ) shows background contributions.

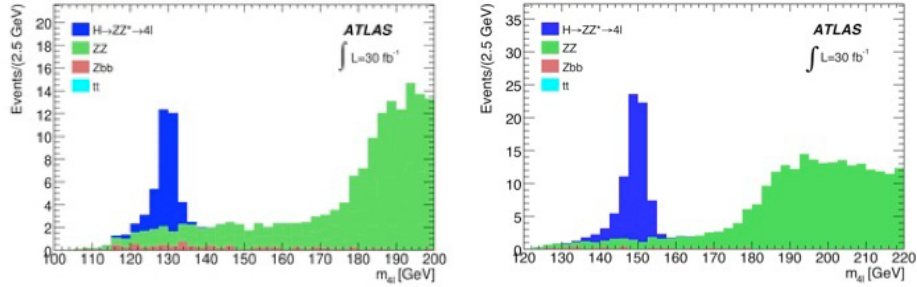


Fig. 8. The invariant mass distribution of  $lll$  with luminosities of  $30\text{ fb}^{-1}$ .  $M(H_{SM}^0)=130$ (a) and  $150$ (b) GeV are assumed.

$H_{SM}^0 \rightarrow \gamma\gamma$  and  $\tau^+\tau^-$  channels have good potential in the mass region lighter than  $130\text{ GeV}$ . For the heavy mass case, ( $\geq 130\text{ GeV}$ ), decay to  $ZZ(\rightarrow \ell^+\ell^-\ell^+\ell^-)$  and  $W^+W^-$  have an excellent performance. After the discovery of the Higgs boson, we can perform to measure the mass and couplings between Higgs and particles with accuracies of about  $0.1\%$  and  $10\%$ , respectively.

### 4.3. Supersymmetry

If the Higgs boson is light, some mechanism to protect Higgs mass from the radiative correction is necessary. Supersymmetric (SUSY) standard models are most promising extensions of the SM, because the SUSY can naturally explain the weak

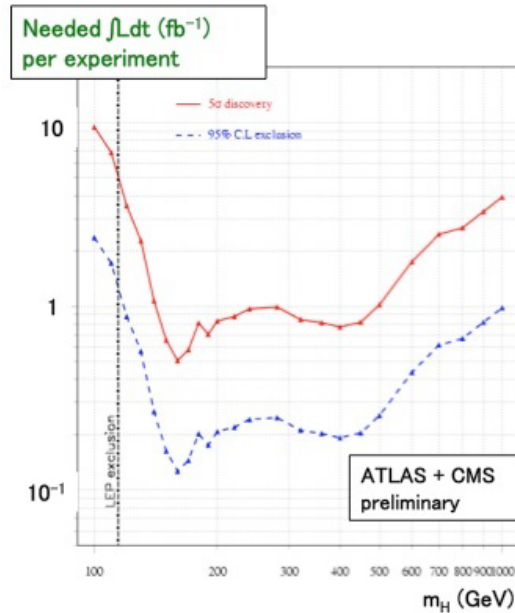


Fig. 9. The needed integrated luminosity as a function of Higgs mass. Red shows  $5\sigma$  discovery and blue shows 95% C.L. exclusion.

boson mass scale. Furthermore, the SUSY models provide a natural candidate of the cold dark matter and they have given a hint of the Grand Unification in which three gauge couplings of the SM are unified at around  $2 \times 10^{16}$  GeV. In SUSY, each elementary particle has a superpartner whose spin differs by  $1/2$  from that of the particle. Discovery of the SUSY particles should open a new epoch of the fundamental physics, which is another important purpose of the LHC project.

#### 4.3.1. Event topologies of SUSY events

$\tilde{g}$  and/or  $\tilde{q}$  are copiously produced at the LHC. High  $p_T$  jets are emitted from the decays of  $\tilde{g}$  and  $\tilde{q}$ . If the R-parity is conserved, each event contains two  $\tilde{\chi}_1^0$ 's in the final state, which is stable, neutral and weakly interacting and escapes from the detection. This  $\tilde{\chi}_1^0$  is an excellent candidate of the cold dark matter. The missing transverse energy ( $\cancel{E}_T$ ), which is carried away by the two  $\tilde{\chi}_1^0$ 's, plus multiple high  $p_T$  jets is the leading experimental signature of the SUSY at the LHC. Additional leptons,  $h(\rightarrow b\bar{b})$  and  $\tau$ , coming from the decays of  $\tilde{\chi}_2^0$  and  $\tilde{\chi}_1^\pm$ , can also be detected in the some part of event.

#### 4.3.2. Inclusive searches

Inclusive searches will be performed with the large  $\cancel{E}_T$  and high  $p_T$  multi-jet topology (no-lepton mode). One additional hard lepton (one-lepton mode) or two same-

sign (SS-dilepton) and opposite-sign leptons(OS-dilepton) can be added to the selections. These four are the promising modes of the SUSY searches, especially no-lepton and one-lepton modes are important for the discovery.

The following four SM processes can potentially have  $\cancel{E}_T$  event topology with jets:

- $W^\pm(\rightarrow \ell\nu) + \text{jets}$ ,
- $Z^0(\rightarrow \nu\bar{\nu}, \tau^+\tau^-) + \text{jets}$ ,
- $t\bar{t} + \text{jets}$ ,
- QCD multi-jets with mis-measurement and semi-leptonic decays of  $b\bar{b}$  and  $c\bar{c}$  with jets

We require at least three jets with  $p_T \geq 50$  GeV, and  $p_T$  of the leading jets and  $\cancel{E}_T$  are required to be larger than 100 GeV. The azimuthal angles between  $\cancel{E}_T$  and the leading three jets are required to be larger than 0.2 for the no-lepton mode to reduce the QCD background. The excess coming from the SUSY signals can be clearly seen in the  $\cancel{E}_T$  distributions as shown in Figs.10 for both no-lepton and one-lepton modes.  $t\bar{t}$  is the dominant background process for the one-lepton mode, and all of the four processes listed above contribute to no-lepton mode.

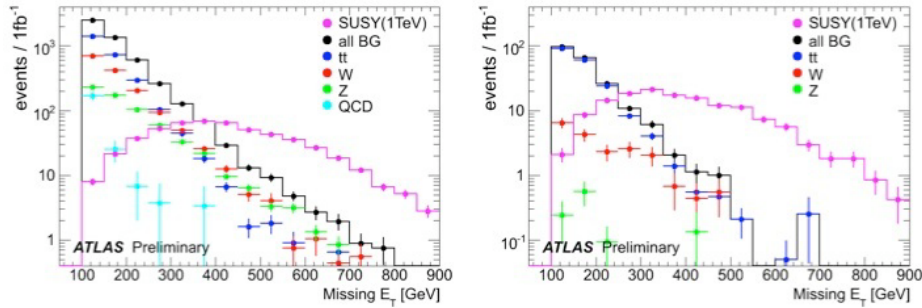


Fig. 10. The  $\cancel{E}_T$  distributions of the SUSY signal and background processes with a luminosity of  $1 \text{ fb}^{-1}$  and  $\sqrt{s}=14 \text{ TeV}$ . (a) No lepton (b) one lepton mode. In both figures, red open histogram show the SUSY signal with  $(m_0=100\text{GeV}, m_{1/2}=400\text{GeV}$  and  $\tan\beta=10)$  The black show the sum of the all SM backgrounds

#### 4.3.3. Discovery potential

Figures 12 show  $5\sigma$ -discovery potential in  $m_0$ - $m_{1/2}$  plane for (a)  $\sqrt{s}=10\text{TeV}$   $L=200 \text{ pb}^{-1}$  and (b)  $\sqrt{s}=14\text{TeV}$   $L=30 \text{ fb}^{-1}$ . Figure 12(a) is corresponding data in 2011, and  $\tilde{g}$  and  $\tilde{q}$  can be discovered upto  $\sim 800$  GeV. No lepton mode has slightly good sensitivity than one-lepton mode. With the naive SUGRA assumption, Chargino and the lightest Neutralino (dark matter candidate) can be discovered upto  $\sim 250$  GeV and 130 GeV, respectively. The interesting region in which

$\Omega_{DM}$  is consistent with the observation is covered in 2011 run. Figure 12(b) is corresponding data in around 2014, and  $\tilde{g}$  and  $\tilde{q}$  can be discovered upto  $\sim 2$  TeV.

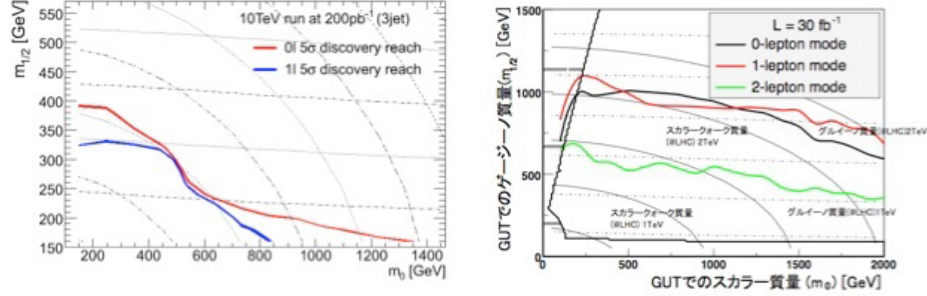


Fig. 11.  $5\sigma$ -discovery potential in  $m_0$ - $m_{1/2}$  plane ( $\tan\beta=10$ ) for (a)  $\sqrt{s}=10\text{TeV}$   $L=200\text{pb}^{-1}$  and (b)  $\sqrt{s}=14\text{TeV}$   $L=30\text{fb}^{-1}$ .

## 5. EWSB scenario 2: Strong Coupling Gauge Theory

Alternative scenario of the EWSB is the Strong Coupling Gauge Theory (SCGT). The di-boson and dilepton resonance are typical event signals at LHC.

### 5.1. $W^+W^-$ and $WZ$ scatter

$W^+W^-$  or  $WZ$  scatters will be affected in the Strong Coupling Gauge Theory. These scatter processes will be observed in VBF processes as shown in Fig.12(a). Chiral Lagrangian model is the effective theory and two parameters of the anomalous coupling ( $\alpha_4$  and  $\alpha_5$ ) are useful for VV scatters. Vector( $\rho$ ) and scalar( $\sigma$ ) resonance masses can be written:

$$M_\rho^2 = \frac{v^2}{4(\alpha_4 - 2\alpha_5)} \quad (1)$$

$$M_\sigma^2 = \frac{3v^2}{4(7\alpha_4 + 11\alpha_5)} \quad (2)$$

Lower mass state is scalar and higher mass is vector resonance. Non-resonance processes are also possible. The differential cross-section of the various resonances(non-resonance) are shown in Fig.12(b). The cross-section is expected to small even at  $\sqrt{s}=14\text{TeV}$ .

The emitted W and Z bosons decay into quark pair or lepton pair ( $W^\pm \rightarrow \ell\nu$   $Z^0 \rightarrow \ell^+\ell^-$ ). Tri-lepton topology ( $WZ \rightarrow \ell\nu\ell^+\ell^-$ ) is the promising channel as shown in Fig.13(a), since the background contribution is expected to be small. But the branching fraction of tri-lepton is also suppressed and the tri-lepton mode is promising only for the lighter case ( $M \sim 500\text{GeV}$ ). For the heavier case ( $M > 800\text{GeV}$ ),

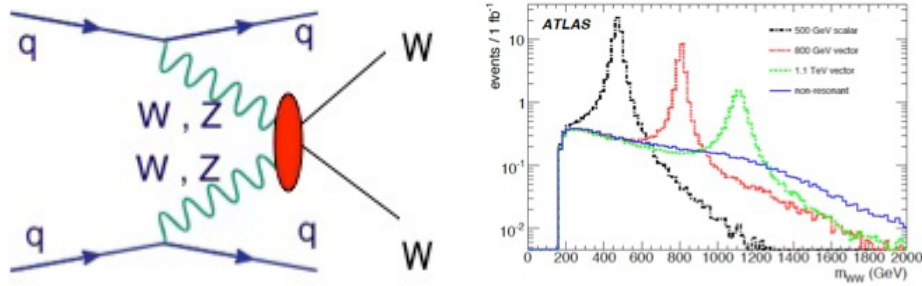


Fig. 12. (a) VBF process for VV scatter (b) di-Boson invariant mass distributions for various models. Scalar and vector resonances (Mass=500,800,1100 GeV) and non-resonance case.

dilepton+jets topology ( $WZ \rightarrow jj\ell^+\ell^-$ ) becomes promising as shown in Fig.13(b) and (c). The integrated luminosity of  $100 \text{ fb}^{-1}$  is necessary for  $M = 500\text{--}800 \text{ GeV}$  resonance case ( $5\sigma$  discovery potential.) More luminosity of  $200 \text{ fb}^{-1}$  is necessary for  $M > 1 \text{ TeV}$  resonance case and it is difficult at LHC for non-resonance case.

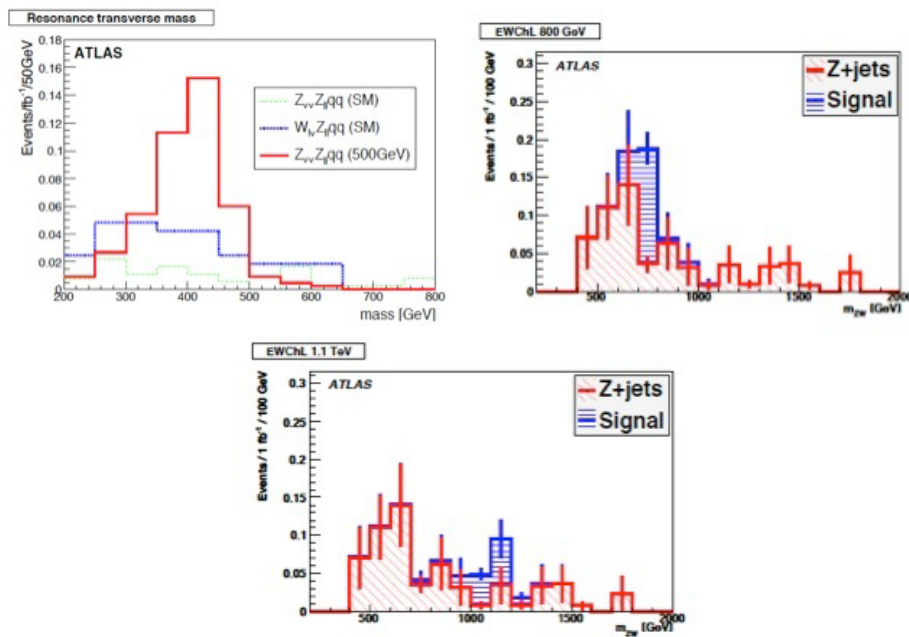


Fig. 13. The invariant mass distribution (a) MT mass for tripleton and missing. The red show the signal of 500GeV scalar. (b) and (c) The invariant mass of  $\ell^+\ell^-qq$  for 800 GeV scalar and 1.1 TeV vector resonance. Blue shows the signal and the red shows the background contributions of  $Z^0 + jets$

### 5.2. Low mass Technicolor model

There might be many TC fermions ( $N_D$ ) to make the walking model, otherwise TC models are strictly conflict with the EW precise measurements at LEP. TC scale  $\Lambda_{TC} \sim 250\text{GeV}/\sqrt{N_D}$  becomes smaller and mass scale of Technicolor particles becomes light.

Nambu-Gladstone-Boson ( $\pi_{TC}$ ) is mixed with  $Z_L$  and  $W_L$ . Technifermion bound state,  $\rho_{TC}$ ,  $\omega_{TC}$  and  $a_{TC}$  will couple with  $W, Z, \gamma$ . They decay into  $VV$  or fermion pair and make the narrow resonance. Mass of these bound state is around 400-800GeV and the decay modes and  $J^{CP}$  are listed in the next table.  $L=10$  or  $5\text{fb}^{-1}$  is necessary for di-boson decay mode and di-lepton decay mode, respectively. These luminosity is expected around 2013 or 2014.

name	$J^{PC}$ Spin	decay mode
$\rho_{TC}^{\pm 0}$	$(1^{--}, I=1)$	$\rightarrow W^+W^-, WZ, ZZ$ $\rightarrow \ell^+\ell^-$
$\omega_{TC}^0$	$(1^{--}, I=0)$	$\rightarrow \gamma Z$
$a_{TC}^{\pm 0}$	$(1^{++}, I=1)$	$\rightarrow \gamma W$ $\rightarrow \ell^+\ell^-$

## 6. Conclusion

LHC is back now and we have real data at  $\sqrt{s}=900\text{ GeV}$  and  $2.36\text{ TeV}$ . The ATLAS and CMS (also ALICE and LHCb) detectors work well and the good performance have been obtained. The LHC will be operated at  $\sqrt{s}=7\text{ TeV}$  for 2010 and 2011 due to the bad connection of splicing. The integrated luminosity is about  $1\text{ fb}^{-1}$  in these two years.

There are two major scenarios for the ElectroWeak Symmetry Breaking:

- (1) light Higgs boson and SUSY
- (2) diboson and dilepton resonance in Strong Coupling Gauge Theory

They can be discovered at LHC before 2013–2015, and we can perform the crucial test.